Royal Netherlands Meteorological Institute
Ministry of Infrastructure and the Environment

TU Delft Delft University of Technology

T2.1-P1: A Seismo-Acoustic Analysis of the 2017 North Korean Nuclear Test

Jelle Assink [1], Gil Averbuch [2], Shahar Shani-Kadmiel [2], Pieter Smets [2] and Läslo Evers [1,2]. Contact: assink@knmi.nl

This work shows that a joint analysis of seismic and acoustic IMS data can be used to quantify seismo-acoustic coupling from the 2017 North Korean nuclear test. Besides the epicentral region, infrasound is coupled from distant regions.

Reference: J.D. Assink, G. Averbuch, S. Shani-Kadmiel, P. S. M. Smets, and L. G. Evers (2018), A Seismo-Acoustic Analysis of the 2017 North Korean Nuclear Test, Seismological Research Letters (2018) 89 (6): 2025-2033. doi: 10.1785/0220180137

Summary

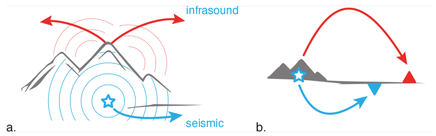

Figure 1: *(a) Partitioning of seismic (blue) and acoustic (red) energy from an underground source. The atmospheric radiation is reduced for deeper buried sources. (b) The radiated infrasound can be detected at long distances from the source, given favorable long-range propagation conditions and low surface wind noise, near the array.*

Underground nuclear tests give rise to seismic and infrasound signals that can be detected on International Monitoring System (IMS) stations. The infrasonic signals are due to seismo-acoustic coupling (Figure 1). The radiation of infrasound is dependent on source depth. Recent studies have demonstrated the added value of seismo-acoustic analyses, for example, to improve depth-yield estimates of (nuclear) explosions.

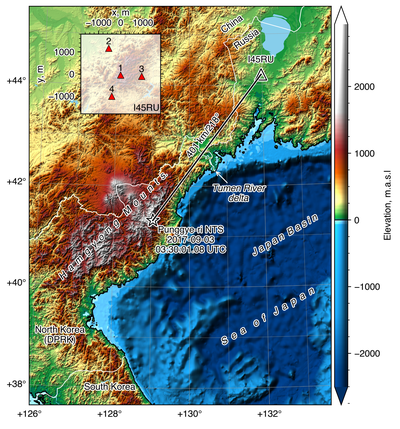

Figure 2: *Shaded relief of surface topography and bathymetry from General Bathymetric Chart of the Oceans (GEBCO) 30 arcsec grid (Weatherall et al., 2015). Punggye-ri nuclear test site (NTS) and event epicenter marked by a star and IMS array I45RU marked by a triangle. The inset frame shows I45RU's array layout.*

In this study, we analyze infrasound recordings from IMS array I45RU in the Russian Federation, at 401 km from the test site (Figure 2). Seismo-acoustic coupling is mapped by applying a back projection technique to the array processing results. We discuss these findings in the context of infrasound propagation conditions during the sixth nuclear test.

Array processing and back projections

Figure 3a and 3b shows array detections in the 0.35-4.0 Hz and 1.0-3.0 Hz bands respectively. The detections between 57-300 s are seismic waves that radiate vertically to the atmosphere, near the array. The arrivals between 1200-1600 s have propagated mostly through the atmosphere and are epicentral infrasound. In the 1-3 Hz band, secondary infrasound is detected between 600-1300 s. Deviations from the test-site azimuth (dashed line) are noted.

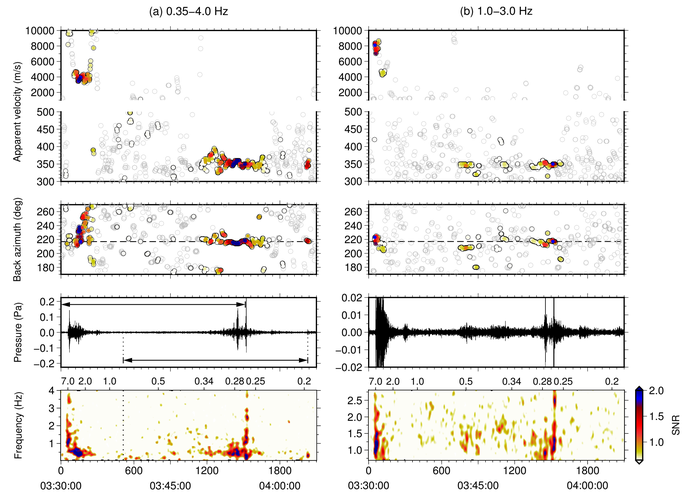

Figure 3: *Array-processing results (a) 0.35-4.0 Hz wideband, and (b) 1.0-3.0 Hz narrowband of I45RU between 03:30:00 and 04:05:00 on 3 September 2017. The frames show the following wavefront parameters as a function of time: apparent velocity, back azimuth, best beam, and coherency as a function of frequency. The color scale indicates the signal-to-noise ratio (SNR) of the detection. Travel time in seconds and celerity (in km/s) are indicated on the lowest frame and are relative to the origin time.*

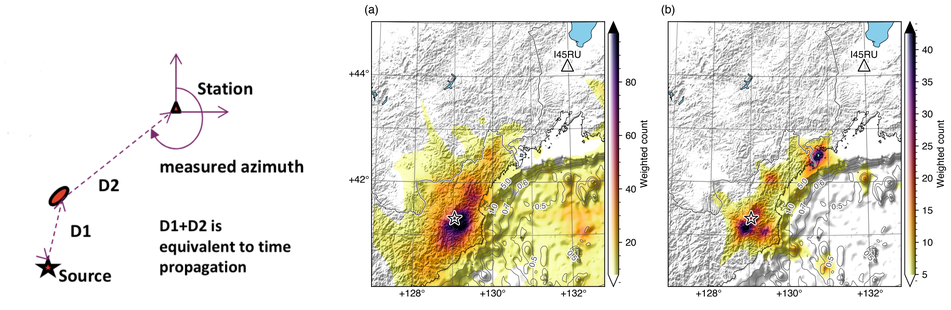

Figure 4: *Backprojection results for (a) 0.35-4.0 Hz and (b) 1.0-3.0 Hz frequency bands overlaid on a topography/bathymetry-shaded relief. Contour lines over the bathymetry correspond to water depth of one acoustical wavelength at the labeled frequency in Hz; evanescent coupling at lower frequencies is expected. The event location, as listed in the Reviewed Event Bulletin (REB), is marked by a star; the I45RU array location is marked by a triangle. Color coding by (SNR) weighted count of detections that originate in each grid cell.*

The estimated traveltime and azimuth can be used to identify locations of seismo-acoustic coupling, by assuming propagation speeds in the earth (path D1; here 6 km/s) and atmosphere (path D2; here 0.28 km/s). The back-projections show that infrasound radiation is not confined to the epicentral region. Distant regions are found to be consistent with locations of topography, sedimentary basins, and underwater evanescent sources, depending on frequency.

Detailed waveform analysis

Figure 5 show (1) an oscillatory wave package, (2) a U-wave with a dominant frequency of 0.1 Hz that can be modeled (blue line) as a thermospheric arrival and (3) a weak arrival that can be associated with the non-tectonic aftershock, having a similar traveltime as arrival (2).

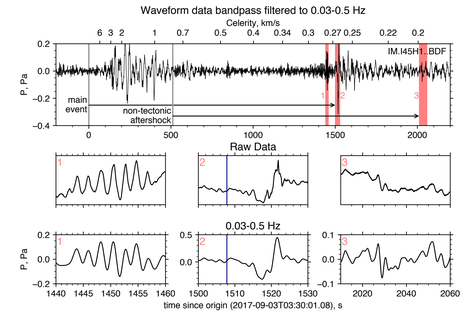

Figure 5: *Detail analysis of individual arrivals at I45H1 relative to the origin time of the explosion. Three time windows marked in red are enlarged in the bottom two rows. The blue vertical line at 1507 s (blue) corresponds to the calculated time of arrival from ray theory.*

Propagation conditions

Not all the arrivals could be explained using propagation modeling with weather forecast models. During the time of the 2017 nuclear test, the middle atmosphere was in transition to the winter state and therefore the horizontal winds in the middle atmosphere were low (Figure 6). During these times, small-scale structure that is unresolved in models influences propagation. Besides a thermospheric refraction (solid line; corr. to signal (2)), infrasound may have scattered from small-scale structures (dashed line; corr. to signal (1)). In addition, propagation along the Earth as well as secondary paths may have contributed to the observations.

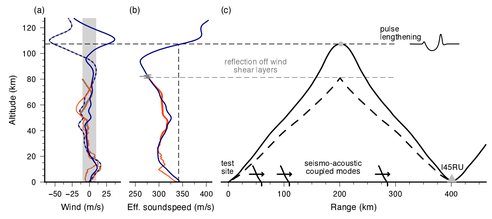

Figure 6: *(left) Atmospheric wind and effective sound speed profiles from HWM14/MSIS00 climatologies (blue) and ECMWF (red) above the test-site around the time of the 2017 test. (right) Resolved (solid) and conceptual infrasound propagation paths that can explain the observations.*

[1] *R&D Department of Seismology and Acoustics, Royal Netherlands Meteorological Institute. PO Box 201, 3730 AE De Bilt, The Netherlands.* [2] *Geoscience and Engineering, Delft University of Technology.*

The contributions by Shahar Shani-Kadmiel, Pieter Smets, and L slo Evers are funded through a VIDI project from the Netherlands Organization for Scientific Research (NWO), Project 864.14.005. Gil Averbuch is funded through the Marie Curie Action WAVES from the European Union within H2020, Grant Number 641943. All authors contributed equally to this work.